



21st IAEA Fusion Energy Conference  
Chengdu, China, 16 - 21 October, 2006

---

IAEA-CN-149/ EX/P8-4

## Characteristic Features of Edge Localized Mode under the Presence of Edge Ergodic Magnetic Field Layer in LHD

S. Morita et al.

NIFS-854

Oct. 2006

## Characteristic Features of Edge Localized Mode under the Presence of Edge Ergodic Magnetic Field Layer in LHD

S.Morita 1), T.Morisaki 1), K.Tanaka 1), M.Goto 1), S.Masuzaki 1), S.Sakakibara 1), K.Narihara 1), K.Ikeda 1), O.Kaneko 1), K.Kawahata 1), A.Komori 1), C.Michael 1), S.Murakami 2) K.Nagaoka 1), S.Ohdachi 1), N.Ohyabu 1), Y.Oka 1), M.Osakabe 1), R.Sakamoto 1), A.Sanin 3), Y.Takeiri 1), T.Tokuzawa 1), K.Toi 1), K.Tsumori 1), L.N.Vyacheslavov 3), K.Y.Watanabe 1), M.Yokoyama 1), O.Motojima 1) and LHD experimental group

1) National Institute for Fusion Science, Toki 509-5292, Gifu, Japan

2) Department of Nuclear Engineering, Kyoto University, Kyoto 606-8501, Japan

3) Budker Institute of Nuclear Physics, 630090, Novosibirsk, Russia

e-mail contact of main author: morita@lhd.nifs.ac.jp

**Abstract.** Existence of the ergodic magnetic field layer surrounding the core plasma argues one of typical characters in Large Helical Device (LHD). A new type of H-mode-like discharges have been obtained at an outwardly shifted configuration of  $R_{ax}=4.00\text{m}$  with extremely thick ergodic layer, where the  $\nu/2\pi=1$  position is located in the middle of the ergodic layer. These H-mode-like discharges can be triggered by changing  $P_{NBI}$  ( $<12\text{MW}$ ) from 3 beams to 2 beams in a density range of  $4\text{-}8\times 10^{13}\text{cm}^{-3}$ , although the spontaneous transition is also observed. ELM-like bursts appeared with a radial propagation of density bursts are occurred at the  $\nu/2\pi=1$  position and are mainly excited at the inboard side of the torus. The frequency of the ELM-like bursts increases with heating power, at which the edge pressure profile is steeper. ELM-like bursts in LHD are briefly interpreted.

### 1. Introduction

Helical plasmas change the performance with appearance of the edge low mode number rational surface at the plasma boundary. This tendency becomes remarkable to the H-mode-like discharges. The H-mode-like phenomena were observed in W7-AS net-current-free ECH plasmas [1] when the major rational surface was positioned near the last closed flux surface (LCFS). Similar H-mode-like discharge were also obtained in CHS NBI discharges [2-4] and Heliotron-J ECH plasmas [5] using the same manner as the W7-AS H-mode by varying the edge rotational transform,  $\nu/2\pi(a)$ .

In LHD, on the other hand, the H-mode-like discharges have been obtained under a high magnetic field of 2.5T in a outwardly shifted magnetic configuration ( $R_{ax}=4.00\text{m}$ ) with extremely thick ergodic magnetic field layer [6,7], whereas the edge transport barrier formed by the H-mode-like discharges have been observed in high- $\beta$  LHD plasmas ( $\beta\sim 2\%$ ) with a low magnetic field ( $B_t<1\text{T}$ ) at  $R_{ax}=3.60\text{m}$  ( $\nu/2\pi(a)=1.56$ ) [8]. In the  $R_{ax}=4.0\text{m}$  configuration the  $\nu/2\pi=1$  position exists in the middle of the ergodic layer. Another interest of this discharge is in the point that periodical H $\alpha$  bursts, which are very similar to the tokamak edge localized mode (ELM), are clearly seen. This ELM-like bursts, however, frequently appears in LHD discharges without such an H-mode-like transition. Similar phenomenon on the ELM-like bursts is also observed in W7-AS and TJ-UU stellarators [9-11]. In this paper characteristics of the ELM-like bursts in LHD are reported with relation to the edge rotational transform, connection length of ergodic magnetic field and H-mode-like transition.

### 2. Edge rotational transform at outwardly shifted configurations

The edge rotational transform at  $\rho=1$ ,  $\nu/2\pi(a)$ , in LHD varies with position of the magnetic

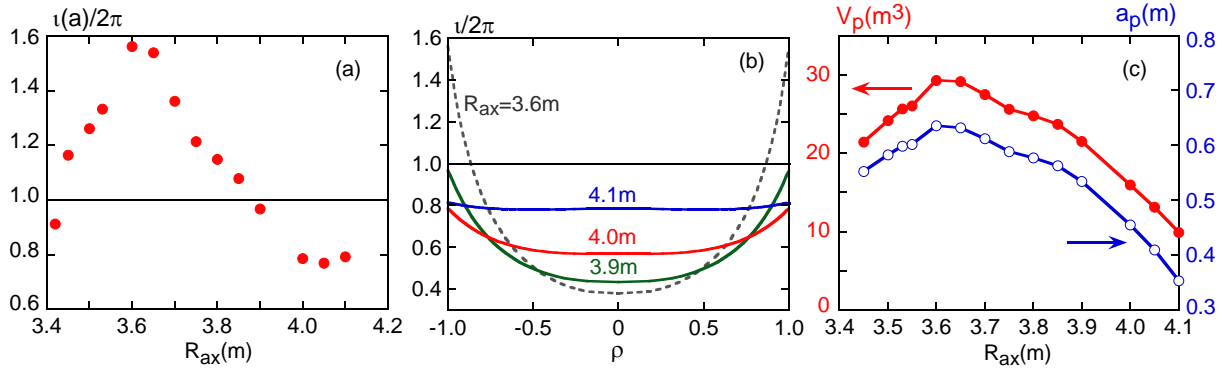


**Fig.1** Edge rotational transform (a), radial profiles of rotational transform (b), and plasma volume  $V_p$  (closed circles) and averaged plasma radius  $a_p$  (open circles) (c).

axis, as shown in Fig.1(a). The values of  $\iota/2\pi(a)$  are below unity at inwardly and outwardly shifted magnetic configurations. However, it is not realistic to operate the LHD at  $R_{ax} < 3.50$  m because of less spatial margin between the plasma edge and the inboard vacuum wall. The operation with low edge rotational transform in LHD is then substantially limited to the plasma axis position of  $R_{ax} \geq 3.90$  m. The profile of rotational transform becomes flat with shifting the  $R_{ax}$  outwardly, as shown in Fig.1(b). As a result, the edge magnetic shear reduces at such outwardly shifted configurations. A clear disadvantage in such low- $\iota/2\pi(a)$  configurations is in the points of small plasma volume and low power deposition of NBI. The averaged plasma radius,  $a_p$ , and the plasma volume,  $V_p$ , are plotted as a function of  $R_{ax}$  in Fig.1(c). The plasma volume at  $R_{ax} = 4.0$  m is a half of the maximum plasma volume at  $R_{ax} = 3.60$  m called 'standard configuration', which gives the best confinement in LHD. The power deposition of tangentially injected NBIs is essentially worse in such outwardly shifted configurations because of the enhanced  $\nabla B$  drift during the beam slowing-down process due to the increase in helical ripple and the deviation of the beam center ( $R = 3.65$ - $3.70$  m) from the plasma center ( $R_{ax} = 3.90$ - $4.10$  m). The absolute value of the plasma performance is, therefore, not better in comparison with the standard configuration.

### 3. Edge magnetic field structures at outwardly shifted configurations

2-dimensional magnetic field structures of the ergodic layer are shown in Fig.2(a) and (b), which are typical examples of thin ( $R_{ax} = 3.60$  m) and thick ( $R_{ax} = 3.90$  m) ergodic layer cases, respectively. The ergodic layer is indicated with the dotted area. Although magnetic field lines connecting to divertor plates called 'divertor legs' are not traced in the figures, X-points as defined in tokamak locate at the right and left ends of the equatorial plane ( $Z = 0$  mm) since two sets of helical coils are positioned at the up and bottom sides of the present horizontally elongated plasma position. The thickness of the ergodic layer becomes minimal at O-points located in up and bottom sides of the figure and the smallest thickness of 1-3 cm is obtained at  $R_{ax} = 3.60$  m. Edge profiles of the magnetic field connection length,  $L_c$ , and the rotational transform are traced at the present horizontally elongated cross-section in (c)-(h) for  $R_{ax} = 3.90$ , 4.00 and 4.10 m cases. Typical ranges of the ergodic layer are indicated by red horizontal bars and the LCFS positions are shown by vertical lines. The ergodic layer in LHD typically consists of chaotic magnetic fields with lengths of 10-2000 m, which correspond to 0.5-100 toroidal turns of the torus. We thus understand the thickness of the ergodic layer is larger at outwardly shifted magnetic axes, and it becomes 30-40 cm at the X-points.

In LHD, the LCFS positions are defined by the outermost flux surface on which the deviation of the magnetic field line is less than 4 mm while it travels 100 turns along the torus

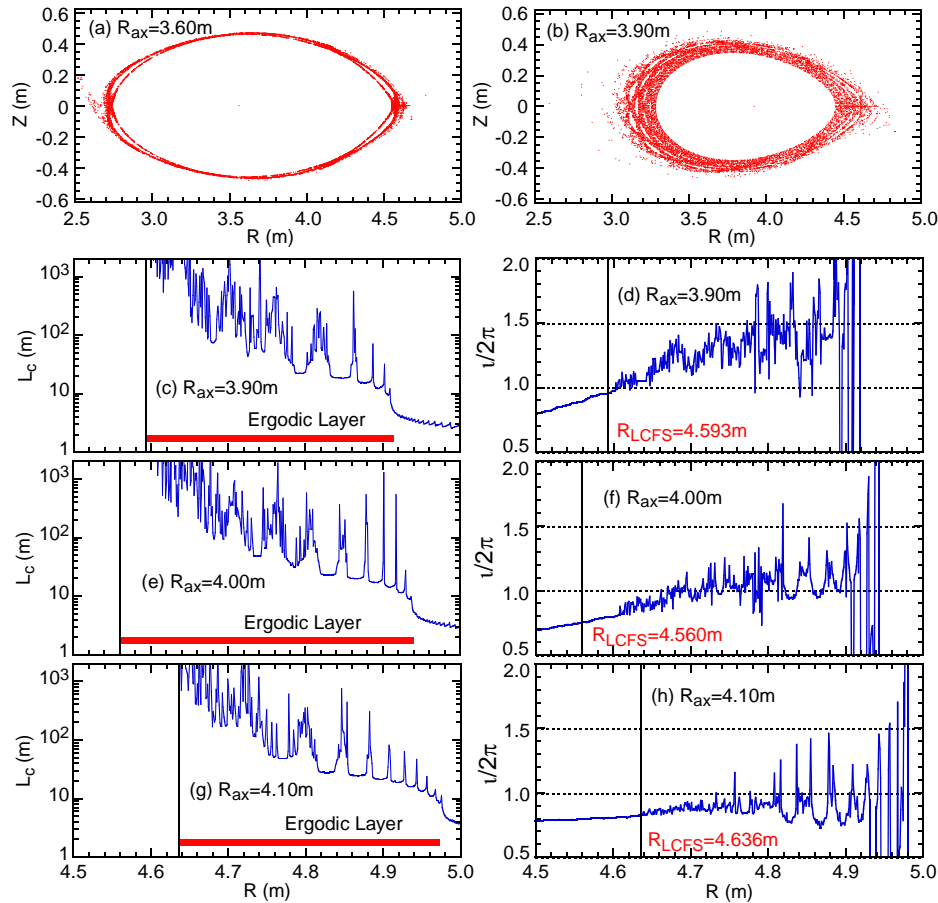


**Fig.2** Magnetic field structures of ergodic layer at  $R_{ax}=3.60\text{m}$  (a) and  $3.90\text{m}$  (b) and edge profiles of magnetic field connection length  $L_c$  ((c)  $R_{ax}=3.90\text{m}$ , (e)  $4.00\text{m}$ , (g)  $4.10\text{m}$ ) and rotational transform  $1/2\pi$  ((d)  $R_{ax}=3.90\text{m}$ , (f)  $4.00\text{m}$ , (h)  $4.10\text{m}$ ). The positions of LCFS are indicated with vertical solid lines.

[12]. The position of the LCFS is, then, affected strongly by the presence of small islands near the outermost flux surface, as appeared in  $R_{ax}=4.00\text{m}$ . The positions of the  $1/2\pi=1$  in  $R_{ax}=3.90$  and  $4.00\text{m}$  are located just near the LCFS and inside the ergodic layer, respectively. Then, the  $1/2\pi=1$  position is  $12\text{cm}$  outside from the LCFS at  $R_{ax}=4.00\text{m}$ , having the magnetic field connection length of  $100\text{m}$ . It should be noticed that any  $1/2\pi=1$  surface does not exist in  $R_{ax}=4.10\text{m}$  case. A variety of electron temperatures of  $10\text{-}500\text{eV}$  are generally observed inside the ergodic layer. The real edge plasma boundary is determined by the competition between heat input and heat loss inside the ergodic layer. Then, the pressure gradient of the  $1/2\pi=1$  position becomes very sensitive to the energy balance in the ergodic layer.

#### 4. H-mode-like discharges

Experimental trials for the discharge improvement have been made among three configurations of  $R_{ax}=3.9, 4.0$  and  $4.1\text{m}$  mainly changing NBI input power and density. An H-mode-like transition was observed at  $R_{ax}=4.00\text{m}$  after quick reduction of the NBI input power while maintaining a relatively high density.

A typical time behavior of discharge with the H-mode-like transition is shown in Fig.3(a)-(c). The discharge built up by  $\text{H}_2$  gas puff is maintained at a middle density of  $n_e=4\times 10^{13}\text{cm}^{-3}$  and one of three NBIs is turned off at  $t=1.25\text{s}$  to trigger the H-mode-like

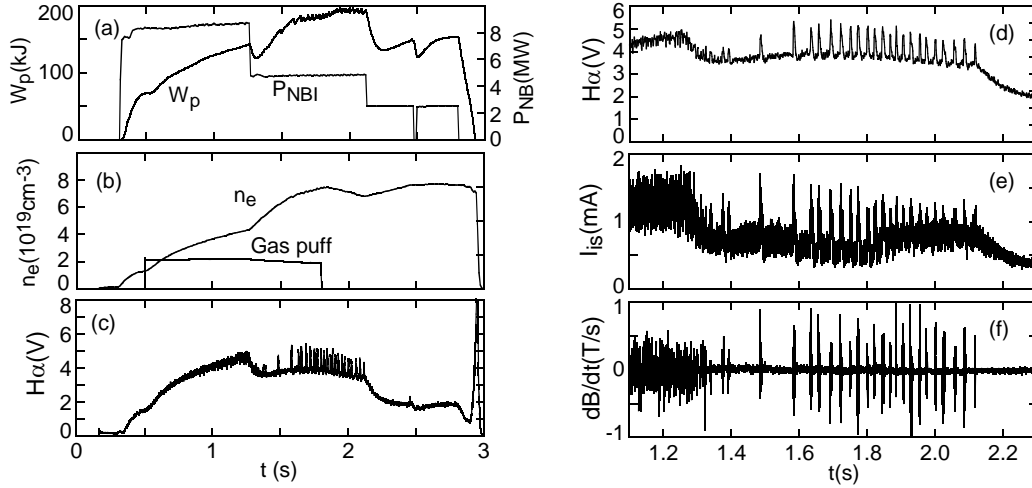


**Fig.3** NBI discharges at  $R_{ax}=4.00\text{m}$  with H-mode-like transition triggered by reduction of NBI power input (left) and extended signals of  $H\alpha$  (d), divertor ion saturation current (e) and magnetic fluctuation (f) (right).

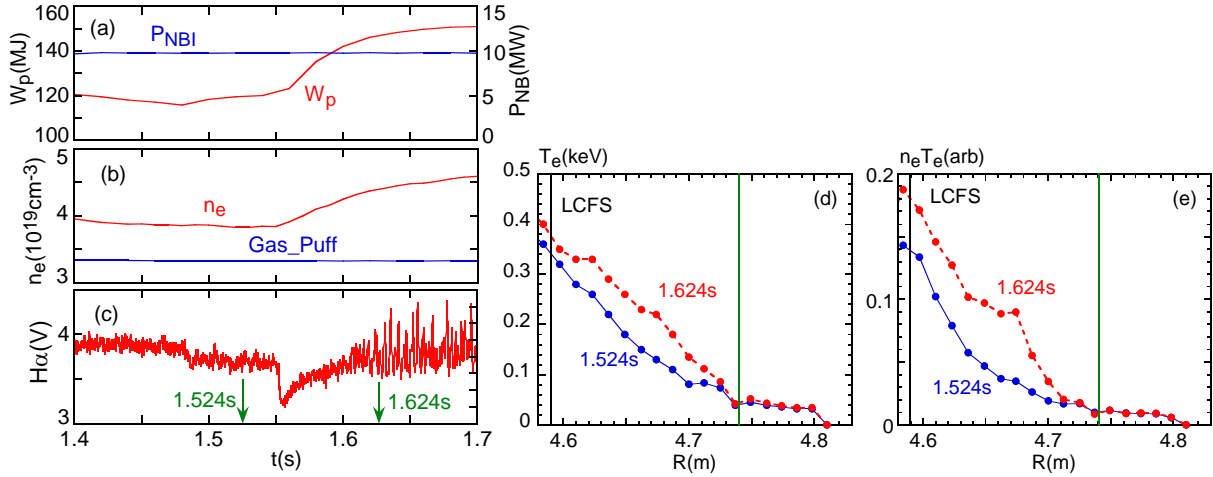


**Fig.4** Spontaneous H-mode-like transition under constant NBI power input and gas puffing rate and radial profiles of edge  $T_e$  (d) and  $n_e T_e$  (e) before ( $t=1.524\text{s}$ ) and after ( $t=1.624\text{s}$ ) transitions.

transition. After turning off the beam line, the  $H\alpha$  emission quickly drops and the density gradually rises, showing a clear transition. ELM-like bursts appear in the  $H\alpha$  signal. Similar bursts are also observed in an electrostatic probe on the divertor plate ( $I_{is}$ ) and a magnetic probe ( $db/dt$ ) as shown in Fig.3 (e) and (f) [6]. The  $H\alpha$  bursts in Fig.3 (d) entirely coincide with the two signals. Reduction of the magnetic fluctuation is also seen after the H-mode-like transition. No clear mode numbers are observed on the ELM-like bursts from the magnetic probe measurement.

This H-mode-like feature, however, disappears after turning off the second NBI at  $t=2.1\text{s}$ . It suggests that the H-mode-like transition needs a relatively narrow power window [13]. The H-mode-like transition cannot be obtained in low- and high-density ranges, appearing only in a density range of  $4\text{-}8 \times 10^{13}\text{cm}^{-3}$  in the present condition. This result indicates that the H-mode transition is sensitive to plasma conditions, especially in a term of  $P_{NBI}/n_e$  ratio. Similar discharges were also tried in the  $R_{ax}=3.90\text{m}$  and  $4.10\text{m}$  configurations. However, any H-mode-like transition with ELM-like bursts was not observed in  $R_{ax}=3.90$  and  $4.10\text{m}$ . This fact strongly suggests the importance in the presence of  $\nu/2\pi=1$  surface in the ergodic layer for

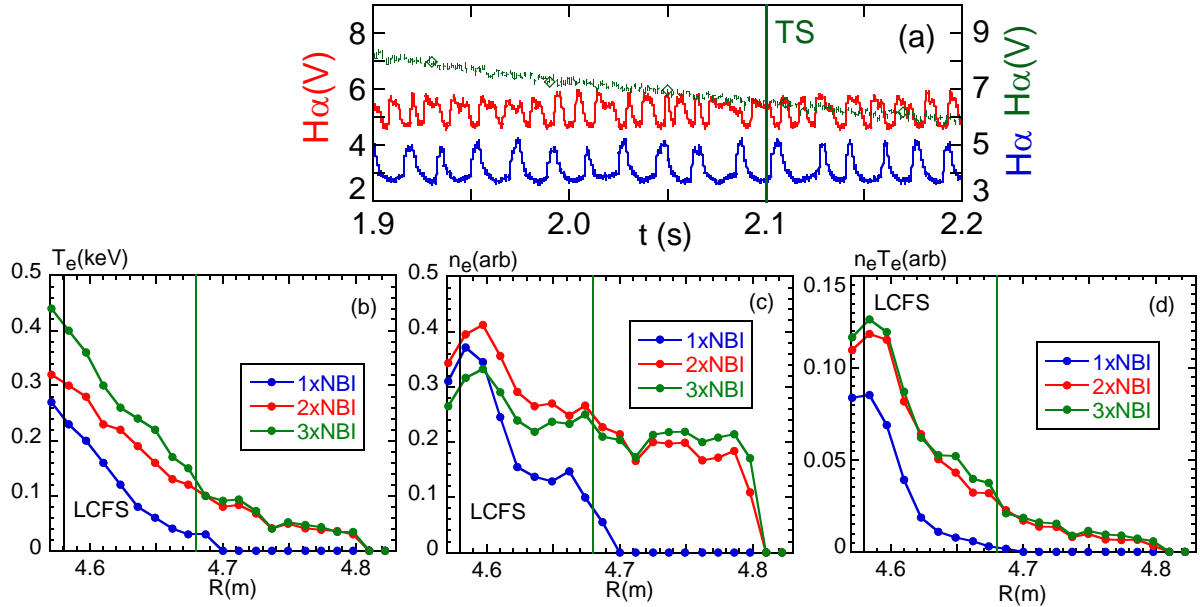


**Fig.5** A variety of ELM frequencies with a parameter of  $P_{\text{NBI}}$  (a) (green: three NBIs, red: two NBIs, blue: single NBI) and edge profiles of  $T_e$  (b),  $n_e$  (c) and  $n_e T_e$  (d).

the H-mode-like phenomenon.

The spontaneous H-mode-like transition is also observed as shown in Fig.4 (a)-(c), although the chance to meet the spontaneous transition is not frequent. The density and plasma stored energy suddenly increase with a reduction of the  $H\alpha$  signal. Time behaviors of all other signals are very similar to the former H-mode-like transition triggered by the  $P_{\text{NBI}}$  change. Temperature and pressure profiles in the ergodic layer measured with YAG laser Thomson diagnostics are shown in Fig.4 (d) and (e), respectively. Solid (blue) and dashed (red) lines indicate the profiles before (1.524s) and after (1.624s) transitions, respectively. Black and green vertical solid lines mean the positions of LCFS ( $R=4.560\text{m}$ ) and  $\iota/2\pi=1$ , respectively. The position of  $\iota/2\pi=1$  is estimated from Fig.2(f). The edge temperature and pressure rapidly increases near  $\iota/2\pi=1$  position and it is seen that steeper temperature and pressure gradients are formed after the transition.

## 5. Characteristics of ELM-like bursts

The frequency of the ELM-like bursts is a function of heating power and electron density. When the density is maintained at a certain level, the frequency is only a function of heating power. Typical examples of ELM-like bursts with different frequencies are shown in Fig.5(a). The green, red and blue lines indicate discharges with three, two and one neutral beam lines for plasma heating, respectively. Each beam line has a similar port-through power of 3MW. It is clear that the frequency of the ELM-like bursts reduces and the amplitude increases when the heating power decreases. Edge temperature, density and pressure profiles during the ELM-like bursts are shown in Fig.5 (b), (c) and (d), respectively. The vertical black and green solid lines indicate the positions of LCFS and  $\iota/2\pi=1$ . The difference between the two and three NBI cases is not clear, although the temperature gradient at  $\iota/2\pi=1$  shows a little difference. However, the profile of the one NBI case is much different from others, especially the density gradient is much steeper and the pressure gradient is much smoother at  $\iota/2\pi=1$ . A temporal change of the edge density and temperature profiles during a single ELM event is necessary in order to understand mechanism on the frequency of the ELM-like bursts.

The frequency and amplitude were also examined by applying  $m/n=1/1$  resonant vertical magnetic field. When the resonant field is additionally applied to the  $R_{\text{ax}}=4.0\text{m}$  configuration, a

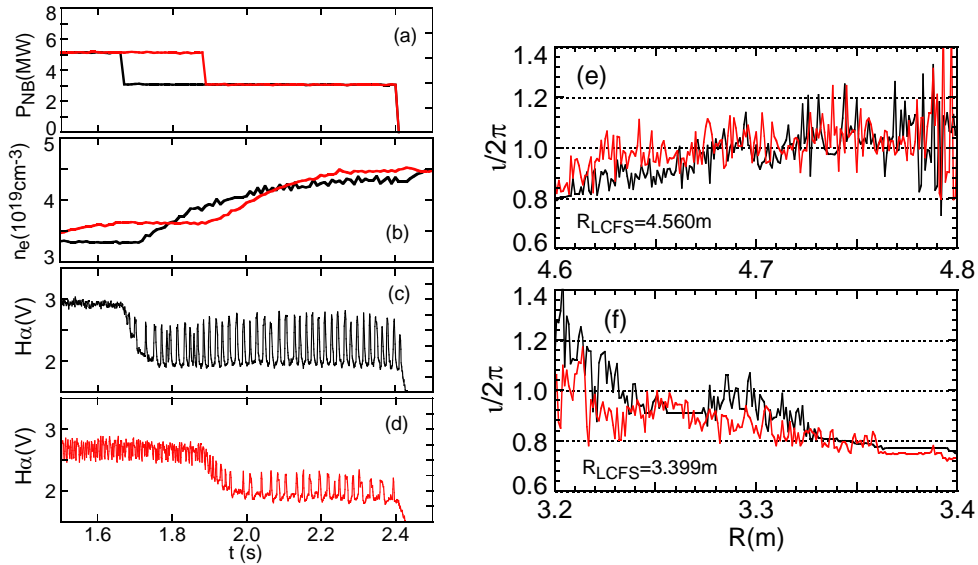


**Fig.6** NBI discharges at  $R_{ax}=4.0\text{m}$  with (red) and without (black) external  $m/n=1/1$  resonant magnetic field.

large modification of the edge rotational transform can not be expected because the  $\iota/2\pi=1$  position exists inside the ergodic layer. The effect of the resonant field application is calculated as shown in Fig.6 (e) and (f). A simple understanding of the figure is not easy, but the application of the resonant field reduces the edge rotational transform and the  $\iota/2\pi=1$  position shifts outside a little. Experimental results are shown in Fig.6 (a)-(d). The frequency of the ELM-like bursts is clearly reduced when the resonant field is applied. As a result, the application of the resonant field leads to the reduction of the pressure gradient at  $\iota/2\pi=1$ .

## 6. Density bursts during ELM-like bursts

Edge density behaviors induced by the ELM-like bursts are analyzed from signals of multichannel interferometer, which measures vertical-chord-integrated densities ( $n_e L$ ) at vertically elongated plasma cross-section. Temporal behaviors of six chord-integrated densities from the edge region are traced in Fig.7(a)-(f) with the rotational transform and connection length (Fig.7 (g), (h)). The ergodic layer at the vertical position in the outwardly shifted magnetic axis position becomes thicker at the inboard side, then, signals of (a) and (b) measure the electron density only from the ergodic layer. A relatively high density is maintained even in the middle of the ergodic layer of  $R=3.399\text{m}$  where the  $L_c$  is roughly 100m. A high density is not formed at a region of  $L_c < 10\text{m}$  (see (f)).

The density bursts are triggered near  $\iota/2\pi=1$  position (see Fig.7(b)) and propagate to both sides with opposite signs like the tokamak sawtooth oscillation. The inversion point can be seen at  $\iota/2\pi \sim 1$  position. The density bursts become remarkable in the inboard side and can be well correlated with the  $H\alpha$  bursts. The positive density pulse toward the outside of the ergodic layer appears at the start by a single ELM-like burst and then the negative density pulse is induced inside the  $\iota/2\pi=1$  position to stabilize the edge density profile. The rise and decay times of the positive pulse are very short compared with the negative pulse. The reason possibly originates in short connection length of the magnetic fields in the ergodic layer.

Precise measurement was tried to investigate the relation between the  $\iota/2\pi=1$  and the density bursts positions using a multichannel  $\text{CO}_2$  interferometer with a spatial resolution of 1cm. The measurement is done also at the vertically elongated plasma cross-section using the same diagnostic port as the above interferometer. The chord-integrated density fluctuation at

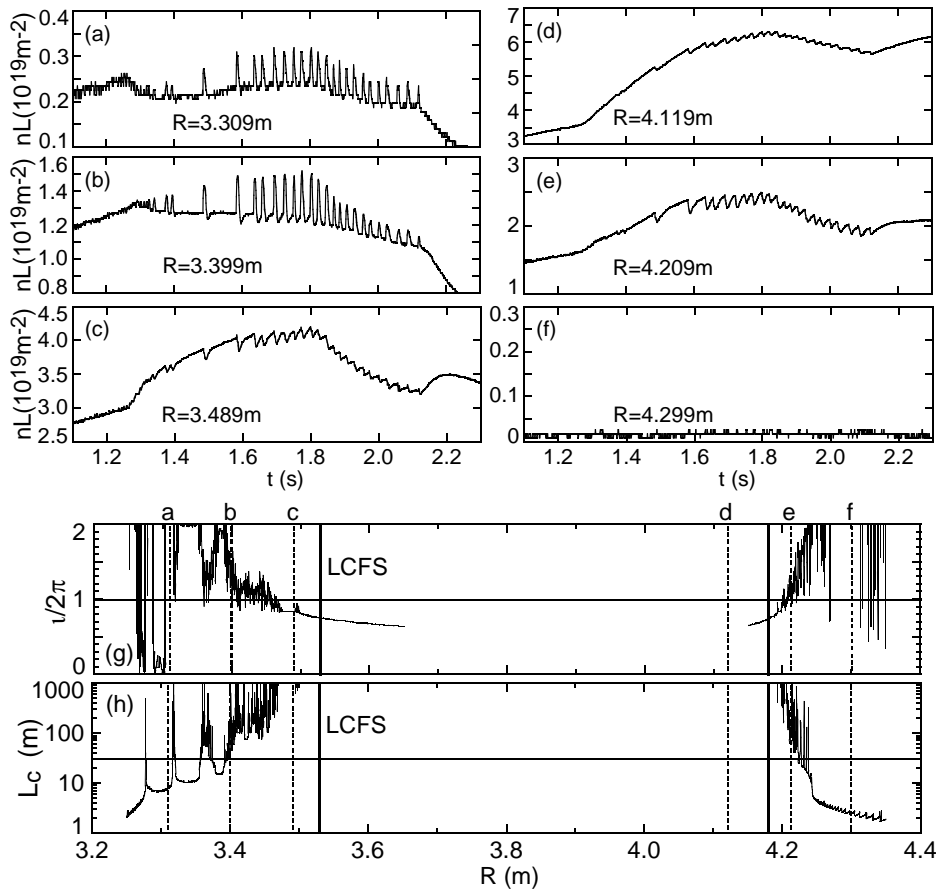


**Fig.7** Density bursts during H-mode-like transition at  $R_{ax}=4.00m$ . Radial positions of chord-averaged densities in (a) to (f) are indicated with vertical dashed lines in rotational transform (g) and magnetic field connection length (h) profiles.

the inboard side induced by the ELM-like bursts is plotted against the measured plasma major radius in Fig.8 (a). Of course, the density bursts observed in all signals are well correlated with the  $H\alpha$  bursts. A peak position of the ELM-induced density fluctuation is seen at  $R=3.46m$ . Edge rotational transform and the magnetic field connection length are also traced for the comparison with the ELM-induced density fluctuation profile in Fig.8 (b) and (c), respectively. It is clearly understood that the peak position of the ELM-induced density fluctuation is consistent with the position of the  $\nu/2\pi=1$  where the  $L_c$  ranges at 100-1000m. This means the ELM-like bursts are triggered at the  $\nu/2\pi=1$  position.

## 7. Summary

H-mode-like discharges have been obtained with the ELM-like  $H\alpha$  bursts in LHD plasmas in outwardly shifted magnetic axis position with a thick ergodic layer, where the  $\nu/2\pi=1$  position is located in the middle of the ergodic layer. A clear density rise and a reduction of magnetic fluctuation were observed. ELM-like bursts also appeared in the density signals with a radial propagation. The ELM-induced density fluctuation profile showed that the ELM-like bursts occur at  $\nu/2\pi=1$  position. The positive density pulse towards the outside plasma edge is observed followed by the negative pulse inside the  $\nu/2\pi=1$  position.

The frequency of the ELM-like bursts increases with the heating power. The edge pressure profile is steeper when the frequency increases. When the heating power exceeds a certain level, the ELM-like bursts disappeared. The ELM-like bursts are mainly excited at inboard side



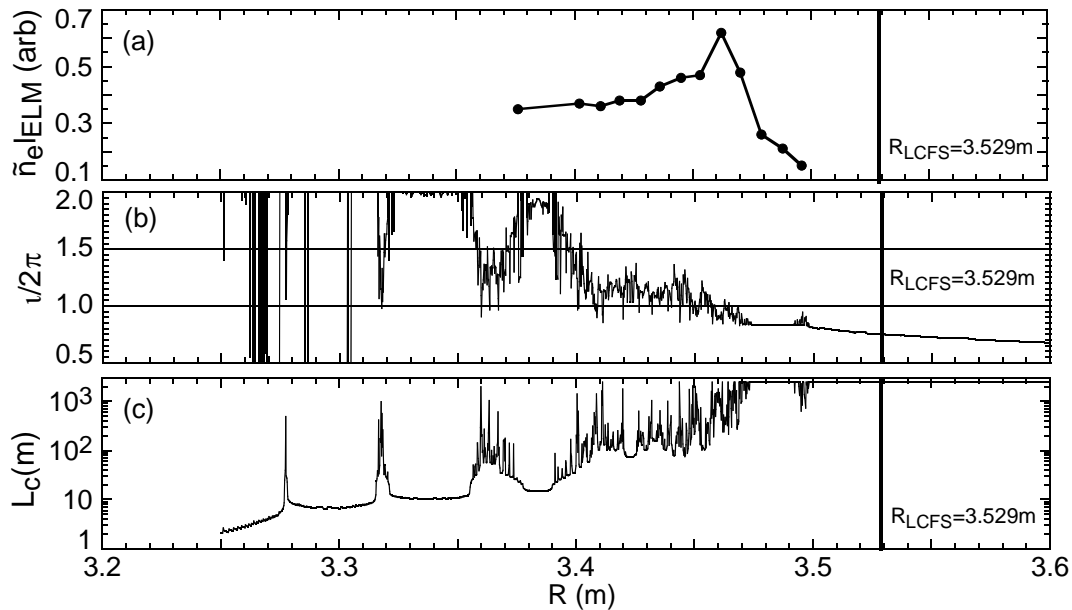


**Fig.8** Precise positions of density bursts measured from CO<sub>2</sub> interferometer with a high spatial resolution of 1cm.

of the torus. Taking into account these experimental results, the existence of an upper power limit on the ELM-like bursts disappearance are similar to tokamak type-III ELM. This gives the same result as the former study of W7-AS and TJ-II [9-11]. However, the frequency dependence on the power input is similar to the tokamak type-I ELM.

On the other hand, the ergodic layer rotational transform calculation indicated in this paper is based on a vacuum magnetic field. Taking into account the plasma pressure, the edge rotational transform profile seems to be modified, based on a modification of chaotic magnetic field structure of the ergodic layer. At present, however, we have no estimation on the effect of the magnetic field modification. This will be a future study.

### Acknowledgments

The authors thank all the members of the LHD team for their cooperation through the LHD operation. This work is partially carried out under the LHD project financial support (NIFS05ULPP527).

### References

- [1] Erckmann, V., et al., Phys.Rev.Lett. **70** (1993) 2086.
- [2] Toi, K., et al., Proc. 14th IAEA Conf. on Plasma Physics and Controlled Nuclear Fusion Research Würzburg **2** (1993) 461.
- [3] Toi, K., et al., Plasma Phys. Control. Fusion **38** (1996) 1289.
- [4] Okamura, S., et al., J. Plasma Fusion Research **79** (2003) 977.
- [5] Sano, F., et al., J. Plasma Fusion Research **79** (2003) 1111.
- [6] Morita, S., et al., J. Plasma Fusion Research **80** (2004) 279.
- [7] Morita, S., et al., Plasma Phys. Control. Fusion **48** (2006) A269.
- [8] Toi, K., et al., Nucl. Fusion **44** (2004) 217.
- [9] Weller, A., et al., Phys. Plasmas **8** (2001) 931.
- [10] Garcia-Cortes, I., et al., Nucl. Fusion **40** (2000) 1867.
- [11] Jimenez, J. A., et al., Plasma Phys. Control. Fusion **48** (2006) 515.
- [12] Morisaki, T., et al., J. Nucl.Mater. **313-316** (2003) 548.
- [13] Morita, S., et al., Proc. 31st EPS Conf. on Plasma Physics London **28G** (2004) P5-103.